

Contents lists available at ScienceDirect

Food Control

journal homepage: www.elsevier.com/locate/foodcont



Quantitative TLC-SERS detection of histamine in seafood with support vector machine analysis



Ailing Tan^{a,b}, Yong Zhao^{a,c}, Kundan Sivashanmugan^a, Kenneth Squire^a, Alan X. Wang^{a,*}

- ^a School of Electrical Engineering and Computer Science, Oregon State University, Corvallis, OR, 97331, USA
- b School of Information Science and Engineering, The Key Laboratory for Special Fiber and Fiber Sensor of Hebei Province, Yanshan University, Qinhuangdao, Hebei, 066004. PR China
- ^c School of Electrical Engineering, The Key Laboratory of Measurement Technology and Instrumentation of Hebei Province, Yanshan University, Qinhuangdao, Hebei, 066004, PR China

ARTICLE INFO

Keywords: Thin layer chromatography Surface-enhanced Raman scattering Machine learning Support vector regression Histamine Seafood allergen

ABSTRACT

Scombroid fish poisoning caused by histamine intoxication is one of the most prevalent allergies associated with seafood consumption in the United States. Typical symptoms range from mild itching up to fatal cardiovascular collapse seen in anaphylaxis. In this paper, we demonstrate rapid, sensitive, and quantitative detection of histamine in both artificially spoiled tuna solution and real spoiled tuna samples using thin layer chromatography in tandem with surface-enhanced Raman scattering (TLC-SERS) sensing methods, enabled by machine learning analysis based on support vector regression (SVR) after feature extraction with principal component analysis (PCA). The TLC plates used herein, which were made from commercial food-grade diatomaceous earth, served simultaneously as the stationary phase to separate histamine from the blended tuna meat and as ultra-sensitive SERS substrates to enhance the detection limit. Using a simple drop cast method to dispense gold colloidal nanoparticles onto the diatomaceous earth plate, we were able to directly detect histamine concentration in artificially spoiled tuna solution down to 10 ppm. Based on the TLC-SERS spectral data of real tuna samples spoiled at room temperature for 0–48 h, we used the PCA-SVR quantitative model to achieve superior predictive performance exceling traditional partial least squares regression (PLSR) method. This work proves that diatomaceous earth based TLC-SERS technique combined with machine-learning analysis is a cost-effective, reliable, and accurate approach for on-site detection and quantification of seafood allergen to enhance food safety.

1. Introduction

Histamine is a biogenic amine that can be produced in fish by bacterial enzymatic decarboxylation of histidine. Histamine fish allergy is one of the most prevalent illnesses associated with seafood consumption in the U.S. constituting 38% of all seafood related food-borne illnesses reported to the US Center for Disease Control (CDC, 2006). The illness is frequently associated with eating fish containing high levels of histamine with a variety of symptoms generally begin with tingling or burning sensations in the mouth followed by the development of rash, nausea, diarrhea, flushing, sweating and headache within a few minutes to 2 h after eating the fish (Bulushi, Poole, Deeth, & Dykes, 2009; Feng, Teuber, & Gershwin, 2016). Fresh fish usually contain negligible amounts of histamine. However, tuna and other pelagic species, which account for significant global fish production, contain large amounts of free histidine in muscles and are more likely to produce histamine as a result of bacterial enzymatic activity if the fish is not properly stored

before consumption (Tarliane, Priscila, Warlley, & Maria Beatriz, 2011). Histamine is colorless and odorless. A high histamine level can exist in fish without noticeable changes in appearance or smell of the fish. Therefore, the rapid and reliable detection of histamine in fish has attracted significant research interest for the sake of public health and safety concerns, as well as for the global fish business. The European Union (EU) and the U.S. Food and Drug Administration (FDA) established a guidance level that the average concentration of histamine in fish for consumption must be lower than 100 ppm and 50 ppm respectively (EC, 2005, pp. 1–25; FDA, 2011, pp. 113–152).

Conventional methods for histamine detection in tuna include high performance liquid chromatography (HPLC) (Önal, Tekkeli, & Önal, 2013), enzyme-linked immunosorbent assay (ELISA) (Lupo & Mozola. 2011), liquid chromatography-mass spectrometry (LC-MS) (Ohtsubo, Kurooka, Tada, & Manabe, 2014) and fluorimetric detection (Muscarella, Lo Magro, Campaniello, Armentano, & Stacchini, 2013) with very low detection limits. However, these methods often require

E-mail address: wang@engr.orst.edu (A.X. Wang).

^{*} Corresponding author.

very expensive instrumentation with time-consuming laborious sample preparation procedures, which are performed by skilled personnel. In addition, these methods can only be used in laboratories. Therefore, there is a need to develop a sensitive, quantitative means for rapid detection of histamine in real tuna samples for on-site inspection to minimize the occurrence of histamine poisoning and enhance seafood safety.

Surface-enhanced Raman spectroscopy (SERS) is one of the most powerful and ultra-sensitive analytical tools, which has been widely applied to food security analysis and many other fields (Craig, Franca, & Irudayaraj, 2013; Gukowsky, Xie, Gao, Qu, & He, 2018; Qi et al., 2013; Zhang et al., 2015). For example, SERS has been reported to successfully determine artificial histamine-spiked fish samples with various types substrates (Gao et al., 2015; Janči et al., 2017) Real-world food samples, however, are complex matrices that generally contain large molecules such as fat and proteins, which may exist strong signal interference or even block the access of the target molecules to the metallic nanoparticles (NPs) surface. Accordingly, some separation techniques have been combined with SERS to address efficient separation, such as liquid chromatography (LC) (Cowcher, Jarvis, & Goodacre, 2014) capillary electrochromatography (CE) (Karaballi, Nel, Krishnan, Blackburn, & Brosseau, 2015), electrostatic separation (ES) (Li, Li, Fossey, & Long, 2010), and thin layer chromatography (TLC) (Freye, Crane, Kirchner, & Sepaniak, 2013; Radu et al., 2016; Zhu, Cao, Cao, Chai, & Lu, 2014), Among these, SERS in tandem with TLC is the most attractive method due to its exclusive advantages such as low cost, simple pretreatment, high throughput, and capability for on-site detection when using portable Raman spectrometers. So far, TLC-SERS has been successfully applied to the separation and identification of various analytes from complex ingredients, such as tobacco-related biomarkers in urine samples (Huang, Han, & Li, 2013), aromatic pollutants in water (Li et al., 2011), natural dyes on works of art (Brosseau et al., 2009), apomorphine in human plasma (Lucotti et al., 2012), ephedrine in dietary supplements (Ly et al., 2015) and so on (Zhang, Liu, Liu, Sun, & Wei, 2014). Recently, Xie, Z. developed a histamine screening method by using Ag NPs and NaCl to obtain SERS spectra of fluram-derivatized histamine on TLC plates (Xie et al., 2017). Gao, F. presented remarkable success in determination of Sudan I in paprika powder using a molecularly imprinted polymers (MIP)-TLC-SERS biosensor (Gao et al., 2015). Yu, W. employed inkjet-printed paper substrates for TLC-SERS to detect melamine in food product (Yu & White, 2013). Nevertheless, in most TLC-SERS methods, the TLC plates are commercially available plates such as silica gel or cellulose, which are usually not SERS-active substrates. The sensitivity and resolution of these reported TLC-SERS was limited. Another challenge is that the low target concentration in complex samples and the multi-step treatment in the TLC-SERS procedure will result in nonlinear relationship between the spectral and the target concentration, which will induce difficulty in quantitative analysis. To overcome this challenge, chemometrics methods such as principal component analysis (PCA) and partial least squares regression (PLSR) have been applied to the TLC-SERS spectral analysis for qualification and quantification (Gao et al., 2015; Liu & Lu, 2017; Lv et al., 2015). However, there have been very few reports using nonlinear multivariate calibration methods, which can account for more measurement variations and provide better quantification accuracy.

Diatomaceous earth is a kind of natural photonic crystal biosilica consisting of fossilized remains of diatoms, which are marine organisms that possess skeletal shells of hydrated amorphous silica, called frustules, with two dimensional periodic pores of hierarchical micro-and nanoscale features (Losic, Mitchell, & Voelcker, 2009; Losic, Rosengarten, Mitchell, & Voelcker, 2006). Diatoms have a variety of eminent properties in optics, physics, and chemistry such as their photonic-crystal nature and high surface-to-volume ratio (nearly $200 \, \mathrm{m}^2/\mathrm{g}$). Hybrid diatom-plasmonic nanoparticle structures have been proved to be excellent SERS substrates for ultra-high performance

biosensors (Kong et al., 2016, Kong, Li et al., 2017, Kong, Squire, Chong, & Wang, 2017, Kong, Xi et al., 2017; Xu et al., 2013). In the previous work of our group, we have demonstrated that diatomaceous earth can function simultaneously as thin layer chromatography to separate toxic molecules from complex food samples and as ultrasensitive SERS substrates to probe the signature Raman peaks using a regular Raman microscope (Kong, Chong, Squire, & Wang, 2018; Kong, Li et al., 2017, Kong, Squire et al., 2017, Kong, Xi et al., 2017). Nowadays, commercial portable Raman spectrometers have been widely available at affordable cost and can achieve similar level of sensitivity compared to regular benchtop Raman microscope, which makes TLC-SERS a feasible method for on-site detection.

In this paper, we demonstrate a diatomaceous earth based TLC-SERS sensing technique combined with machine learning analysis to quantitatively detect seafood allergen in real spoiled tuna samples. We fabricate a diatomaceous earth TLC plate as a separable SERS-active substrate to detect histamine in artificially spoiled tuna solution down to 10 ppm by a BW&TEK portable Raman spectrometer. Support vector machine is a multivariate calibration method based on statistical learning theory and is very powerful in spectroscopy analysis applications owing to its nonlinear characteristics (Dong, Weng, Yang, & Liu, 2015; Wu et al., 2015). Recently, Hu, X. et al. reported a TLC-SERS technique to screen pericarpium papaveris in hot pot condiments using Support vector machine qualification analysis based on first derivative spectra, claiming 100% screening accuracy (Hu, Fang, Han, Liu, & Wang, 2017). However, no quantitative results were obtained and no discussion of detection limit was included in this report. Herein, we applied principal component analysis (PCA) and support vector regression (SVR) to quantitatively analyze the TLC-SERS spectral data of real tuna samples that spoiled at room temperature for 0, 4, 8, 12, 24, 36 and 48 h. PCA was used to extract key features as the input for the SVR model. Compared to traditional linear PLSR model, the PCA-SVR method achieved more accurate quantitative prediction. To the best of knowledge, this is the first attempt to combine TLC-SERS sensing technology with nonlinear regression machine learning method of SVR for quantitative analysis. Our experimental results proved that an SVRenabled TLC-SERS device, which can be measured by a portable Raman spectrometer, would enable a rapid, cost-effective, reliable, and quantitative on-site sensing method to detect trace level of seafood allergen, and potentially many other targets in complex real biological samples.

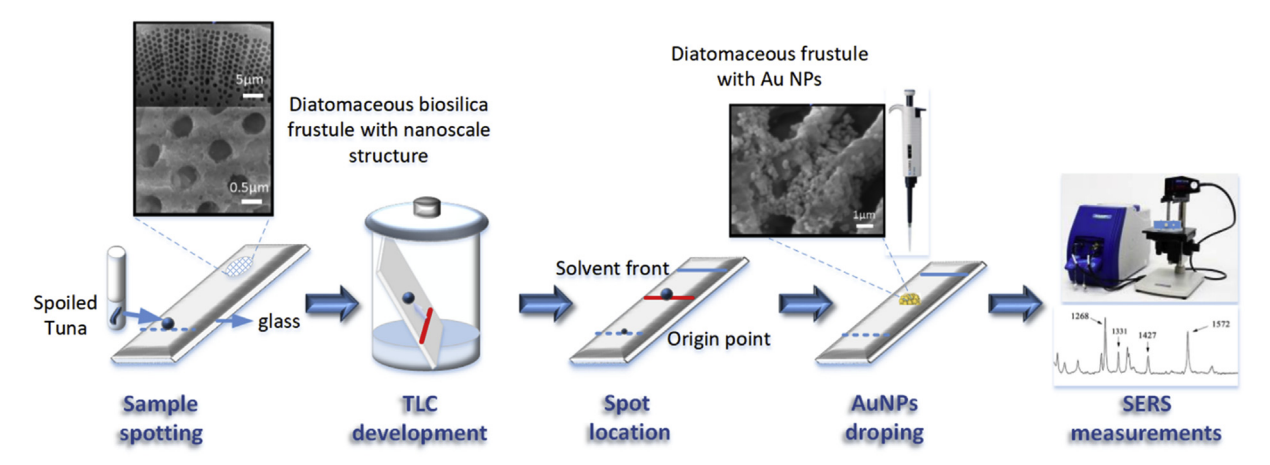
2. Materials and methods

2.1. Materials and reagents

Diatomaceous earth, sodium carboxymethyl cellulose and histamine (purity > 97.0%) were purchased from Sigma-Aldrich. Tetrachloroauric acid (HAuCl₄) was obtained from Alfa Aesar. Trisodium citrate (Na₃C₆H₅O₇), anhydrous ethanol, ammonium hydroxide (NH₄OH, 28%) were purchased from Macron. Trichloroacetic acid (crystalline) was obtained from Fisher Chemical. Tuna meat was purchased from local supermarkets. The chemical reagents used were of analytical grade. Water used in all experiments was deionized and further purified by a Millipore Synergy UV Unit to a resistivity of $18.2\,\mathrm{M}\Omega$ cm.

2.2. Fabrication of diatomaceous earth TLC plates

The diatomaceous earth TLC-SERS plates were fabricated by spin coating on glass slides. The diatomaceous earth was first dried at 150 °C for 6 h in an oven, after cooling to room temperature, 12 g of diatomaceous earth was dispersed in 20 mL of 0.5% aqueous solution of carboxymethyl cellulose and then spread on the glass slide by spin coating at 800 rpm for 20 s. In order to improve the adhesion to the glass slides, the plates were placed in the shade to dry and then activated at 110 °C for 3 h.



Scheme 1. Schematic representation of the diatomaceous earth TLC-SERS detection of seafood allergen from real tuna samples using portable Raman spectrometer.

2.3. Preparation of Au NPs

All glassware used in the Gold nanoparticles (Au NPs) prepare process was cleaned with aqua regia (HNO₃/HCL, 1:3, v/v) followed by washing thoroughly with Milli-Q water. Au NPs were prepared using sodium citrate as the reducing and stabilizing agent according to the literature (Grabar, Freeman, Hommer, & Natan, 1995). Briefly, a total of 100 mL of 1 mM chloroauric acid aqueous solution was heated to the boiling point under vigorous stirring. After adding 4.2 mL of 1% sodium citrate, the pale yellow solution turned fuchsia quickly. The colloids were kept under reflux for another 20 min to ensure complete reduction of Au ions. After cooling to room temperature, the colloids were centrifuged at 9000 rpm for 15 min.

2.4. TLC-SERS method

Scheme 1 shows the procedure of the diatomaceous earth TLC-SERS method for the detection of histamine from tuna fish samples. We processed fresh tuna meat immediately after purchasing from a local super market. The tuna meat was first completely grinded by a blender and a homogenizer. For artificial histamine-spiked tuna solution preparation, 2 g blended tuna meat were mixed with 10 ml trichloroacetic acid (10%) with ultrasonic extraction for 3 min and then the samples were spun in a centrifuge at 6000 rpm for 5 min. 2 μL supernatant was mixed with 2 μL of histamine-water solutions by a pipette. For real spoiled tuna samples with different spoilage time, every 2 g blended meat was transferred to a falcon tube. They were sotred at room temperature for 0, 4, 8, 12, 24, 36 and 48 h respectively. After these tuna samples were spoiled, the same ultrasound and centrifuge processes were conducted and 50- μL supernatant was taken for TLC-SERS experiment.

Then, 1- μ L liquid was spotted using a micro-pipette at 12 mm from the edge of the diatomaceous earth TLC plate. After drying in air, the TLC plate was kept in a TLC development chamber with mobile phase eluent for 10 min and then the TLC plate was dried in an oven for 1 min. Pauly's reagent visualization was used to show the histamine spot on the TLC plate (Tao et al., 2011). The retention factor (R_f) of the analyte on the TLC plate was calculated and marked so that the analyte spot could be traced even when they are not visible at low concentrations. Next, 2 mL solution of concentrated Au NPs were deposited on the spot by drop casting. A portable Raman spectrometer with an excitation laser wavelength of 785 nm was used to obtain the SERS signals. The laser power, the scanning range, the optical resolution, and the integration time were set as 30 mW, 500-1800 cm $^{-1}$, 2 cm $^{-1}$, and 5000 ms respectively. Each SERS measurement was averaged three times.

2.5. Instrumentation

BWS465-785S portable Raman spectrometer equipped with a 785 nm excitation wavelength of Globar source (BW&TEK Inc) was used for acquiring SERS spectra. Diatomaceous earth TLC plates were fabricated using a MTC-100 vacuum spin coater. UV–vis absorption spectra were recorded by a NanoDrop 2000UV–Vis spectrophotometer (Thermo Scientific) using polystyrene cells of 1 cm optical path. Scanning electron microscopy (SEM) images were acquired on FEI Quanta 600 FEG SEM with 15–30 kV accelerating voltage. Quintix24-1s Sartorius quintix, isotemp stirrer, fisher mini vortexer and sorvail legend X1 centrifuge (Thermo Scientific) were also used in the experiments.

2.6. Support vector regression and spectral data analysis

Machine learning algorithms were applied to resolve the interference in the SERS spectra due to intrinsic random natures of both the TLC process and SERS measurement. PCA is a powerful multivariate statistical technique which has been widely used in SERS sensing for dimension reduction and feature extraction for spectral analysis (He et al., 2011; Jarvis, Brooker, & Goodacre, 2004). The PCA method reduces data redundancy and produces a new set of orthogonal variables called principal components and projects the original data into the lower-dimension principal component feature space, which accounts for most of the variance and the key information of the original data simultaneously.

For the quantitative analysis, PLSR is a basic tool for modeling the linear relationship between the digitalized spectra data and the interesting chemical index in chemometrics. However, the TLC-SERS spectra of complex real tuna samples may be affected by many nonlinear factors, which makes nonlinear analytical methods more effective. SVR is an ideal supervised learning algorithm used for nonlinear regression based on support vector machine. The main principal of SVR is briefly described as follows: first, the raw data is mapped onto a higher dimensional feature space using the kernel functions, which is a nonlinear mapping function. Then, with the application of mathematical optimization methods, the linear regression is performed in the higher dimensional feature space. Finally, the regression function in the higher dimensional space is back-transformed into the initial data space and used to explain the nonlinear relationship. The most important parameters for SVR are the kernel function and the parameter controlling the priority of the size constraint of the slack variables. In this study, we used radial basis function (RBF) as the kernel function (Krooshof, Üstün, Postma, & Buydens, 2010), which is defined as $\exp(-\gamma |u-v|^2)$, where u and v are the two generic sample data vectors. Parameter γ and the penalty factor C, which was used for preventing over-fitting, were determined by grid searching algorithm for optimal values. We

performed 5-fold cross-validation method to build the calibration model. For each spoilage time, we randomly chose a set of 16 TLC-SERS spectra for each spoiled time group to serve as the training dataset (112 spectra in total) and selected another 4 spectra (28 spectra in total) to form the testing dataset. We also built a PLSR model for the comparison with the nonlinear SVR model.

Model performance was assessed for the training and testing dataset and compared based on four criteria that are squared correlation coefficient ($\rm R^2$), root-mean-square error of cross-validation (RMSECV), rootmeansquare error of prediction (RMSEP) and ratio of prediction deviation (RPD). RPD is the ratio of standard deviation of RMSEP. The RPD value accounts for the natural variation in the data to the size of prediction errors obtained in the model, which is useful to interpret the prediction efficiency of the model. An accurate model should have low RMSEC and RMSEP values, high $\rm R^2$ and RPD.

All data processing and chemometrics algorithms were performed with MATAB R2018a (MathWorks Inc., Natick, MA, USA). The PCA and PLSR used the functions in MATLAB. The SVR regression model was developed by the free LIBSVM toolbox that originally developed by Zhiren Lin, Taiwan (accessible at http://www.csie.ntu.edu.tw/cjlin/libsvm).

3. Results and discussion

3.1. Characterization and evaluation of Au NPs-decorated diatomite substrates

The morphology of a single diatomaceous earth and the diatomaceous earth layer on the glass substrate were characterized by SEM (Fig. S1), which indicate that the main component of the stationary phase on the TLC plate is disk-shaped diatomite biosilica with honeycomb structure. The highly porous structure with uniform pore size ($< 100 \, \mathrm{nm}$) of the diatomaceous earth has low fluid flow resistance so it enables more homogenous fluid flows into the pores, which can perform smooth and uniform eluent migration during the TLC development.

The UV–vis absorption spectroscopy of the prepared gold colloidal nanoparticles was shown in Fig. S2. The localized surface plasmon resonance peak is at about 528 nm with a narrow bandwidth, which indicates their diameters are approximately 40 nm. According to the basis of the Lambert's law based on UV–vis spectroscopy, the concentration of Au nanoparticles was calculated to be about 4 \times 10 $^{-10}$ M with a molar extinction coefficient of 3.4 \times 10 10 M $^{-1}$ cm $^{-1}$. Fig. S3 presented the SEM image of the diatomaceous frustules with Au NPs, which can serve as high performance SERS substrates as our group has reported previously (Kong et al., 2016).

3.2. TLC-SERS analysis of mixed histamine-tuna using portable Raman spectrometer

The first step is to determine the characteristic Raman peaks of histamine by measuring the SERS spectra of histamine in water solution and in tuna extract using our portable Raman spectrometer. The SERS spectra measured from standard histamine-water solution is shown in Fig. 1(a). There are several clear histamine Raman peaks at 1264, 1302, 1313 and 1571 cm⁻¹, which are assigned to imidazole ring stretching and breathing (Davis, McGlashen, & Morris, 1992; Ramírez, Collado, & Silla, 2003). The measurement results are in good agreement with the work of Tibor et al. (Janči et al., 2017). There are some small variations of wave numbers (less than 2 cm⁻¹), which can be caused by equipment calibration or difference of experimental conditions.

Next, we prepared artificial histamine-spiked tuna solution and measured the SERS spectra with histamine concentration ranging from 10 to 500 ppm by the portable Raman spectrometer. From the SERS spectra shown in Fig. 1(b), we can clearly observe the peaks at 721, 1362 and $1454\,\mathrm{cm}^{-1}$, which are not associated with histamine.

However, the peaks at 1302 and 1571 cm⁻¹ may come from histamine but with much larger spectral width. This is understandable because real tuna meat contains complex components such as proteins, Amino acid, DNAs, and tissue particles, which may induce strong interference signals and block the access of histamine molecules to the plasmonic NP surface.

Fig. S4 shows the SERS spectra of standard histamine-water solution (concentration of histamine: 500 ppm), the fresh tuna extract solution and artificial histamine-spiked tuna solution (final concentration of histamine: 500 ppm). Indeed, the comparison in Fig. S4 shows that the main characteristic Raman peaks of the tuna meat extract in the artificial histamine-spiked samples can create significant interference to histamine sensing. Therefore, it is difficult to determine the presence of histamine directly from the histamine-tuna mixture, which suggests that TLC separation of histamine from the tuna sample is essential for the measurement.

The TLC separation is conducted according to the procedure as described in Section 2.4. A mixture of ethanol and ammonia (v/ v = 3:1) was used as the mobile phase eluent. The developed TLC plate was treated with Pauly's reagent and then heated to visualize the spots (Fig. S5). The SERS spectra of the artificial histamine-spiked tuna samples (final histamine concentrations: 500, 200, 100, 50 and 10 ppm) after performing TLC developments were shown in Fig. 2. The feature peaks of histamine at 1264, 1313 and 1571 cm $^{-1}$ were clearly observed, which proves that the diatomaceous TLC plate can successfully separate histamine from artificial histamine-spiked tuna mixture. The characteristic bands exhibited monotonous decrease in intensity as the mixture concentration decreases and the detection limit of histamine concentration is as low as 10 ppm.

Fig. S6 compares the SERS spectra of artificial histamine-spiked tuna solution (final concentration of histamine: 500 ppm) before and after TLC separation. With the diatomaceous plate TLC separation, the peaks of tuna components at 721, 1362 and 1454 cm⁻¹ disappeared or are significantly reduced in intensity. Meanwhile, the featured SERS peaks of histamine are promoted, which correlate well with the SERS spectra in the standard histamine-water solution.

3.3. TLC-SERS screening of histamine in real spoiled tuna samples

As a comparison, direct SERS sensing without TLC was also conducted for each spoiled tuna sample. The SERS spectra without and after TLC development were shown in Fig. 3 (a) and (b) respectively. It can be clearly seen from the spectra comparison that the feature Raman peaks of histamine were weak or obscured of spoiled tuna samples without performing TLC development. The peak at 721 cm⁻¹ is assigned to the amino group (-NH₃⁺) deformation vibration and the $1454\,\mathrm{cm}^{-1}$ is associated with the C–H deformation vibration of protein. During the spoilage process, not only histamine is produced, but also the concentration of amino groups increases due to tuna meat decomposition. Therefore, regular SERS will detect the peaks related to both histamine and amino groups as shown in Fig. 3(a). These peaks will have the same increasing trend as the spoilage time increases. However, after TLC separation, the interference peaks of 721 and 1454 cm⁻¹ disappeared as shown in Fig. 3(b) as the amino groups are separated, and the 1313 and 1571 cm⁻¹ Raman peaks of histamine were clearly observed though were not very sharp, while the 1264 cm⁻¹ Raman peak is less prominent compared with the SERS spectra from the histamine-spiked tuna solution. We collected the SERS spectra of 0 h spoilage time sample, that is, the fresh tuna meat sample containing no histamine. For such fresh sample, no histamine signature peaks can be found as shown in Fig. 3. When the spoilage time increases, the histamine signature peak starts to appear and the intensity also increases. This proves from another angle, that the 1313 and 1571 cm⁻¹ peaks cannot come from the natural ingredients from fresh tuna.

The spectra for fresh tuna supernatant, standard histamine-water solution (500 ppm) and supernatant from the tuna spoiled for 24 h

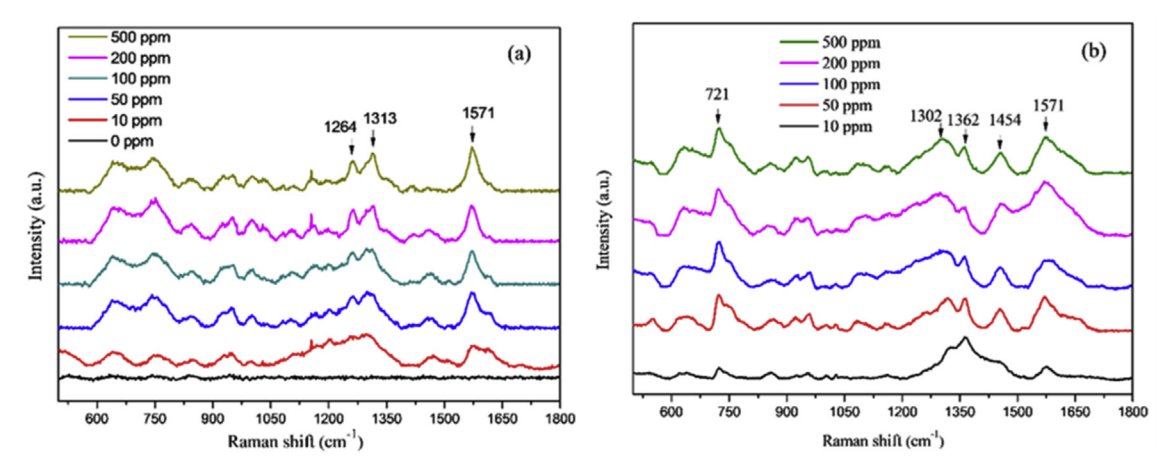


Fig. 1. (a) SERS spectra of standard histamine-water solution at different concentrations; (b) SERS spectra of artificial histamine-spiked tuna solution at different concentrations

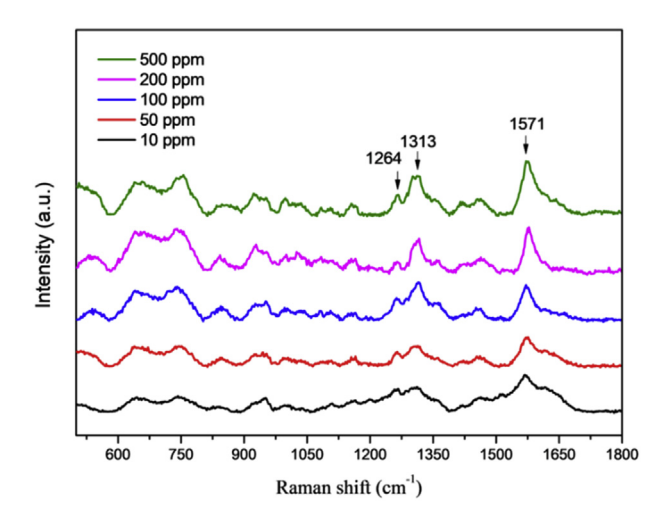


Fig. 2. TLC-SERS spectra of artificial histamine-spiked tuna solution with different histamine concentrations.

without and after TLC procedure were all shown in Fig. S7. The peaks and shape of the SERS spectra between the TLC-SERS result and the standard histamine solution are relatively consistent. The 20 SERS spectra of tuna sample spoiled for 24 h without TCL and with TLC were shown in Fig. S8, which shows reasonable repeatability but with certain level of variation. Therefore, it is very convincing to conclude that TLC

suppresses the interference from real food matrix efficiently and TLC-SERS method can directly provide qualitative screening of histamine from real spoiled tuna samples.

3.4. Quantitative analysis of histamine level in real spoiled tuna samples

In order to quantitatively analyze the histamine level in spoiled tuna samples, we first conduct a simple univariate analysis. For the measured samples, we plotted the intensity of the two feature Raman peaks of histamine at $1313\,\mathrm{cm}^{-1}$ and $1571\,\mathrm{cm}^{-1}$ with standard error versus the spoilage time as shown in Fig. 4. It can be seen that the intensity of these two characteristic peaks with TLC development is significantly higher than that of the samples without the TLC procedure. In addition, there is better correlation between the Raman peak intensity and the spoilage time using TLC-SERS. Overall speaking, the intensity will increase as the spoilage time is longer. While for the data without TLC procedure, the trend is not clear.

It can also be seen from Fig. 4 that the standard error of the Raman peak intensity of samples with TLC development is relatively large, which comes from the intrinsic random natures of both the TLC process and SERS measurement. From such simple univariate analysis, it is difficult to obtain accurate quantitative results due to the poor linearity between the Raman peak intensity versus the spoilage time. Therefore, nonlinear chemometrics methods should be used to determine the spoilage time of real tuna samples, which can be used to evaluate the allergen level.

For further spectral analysis, PCA was first carried out to extract the

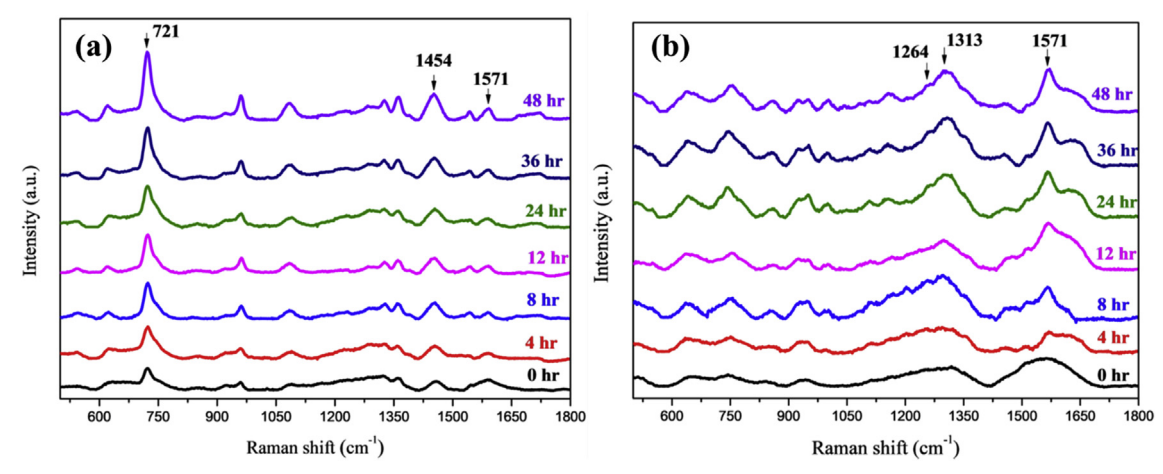


Fig. 3. (a) SERS spectra of real spoiled tuna samples at different spoilage hours without TLC; (b) after conducting TLC development.

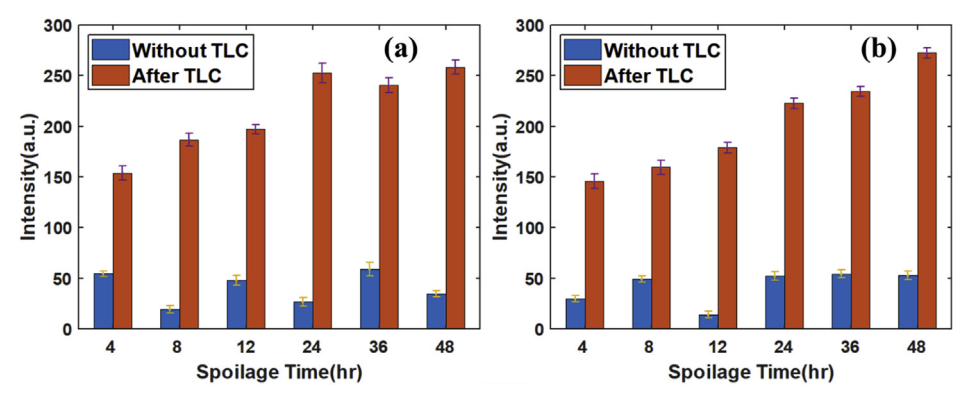


Fig. 4. (a) Intensity distribution of the SERS spectra of six different spoilage time at $1313\,\mathrm{cm}^{-1}$ peak; (b) at $1571\,\mathrm{cm}^{-1}$ peak.

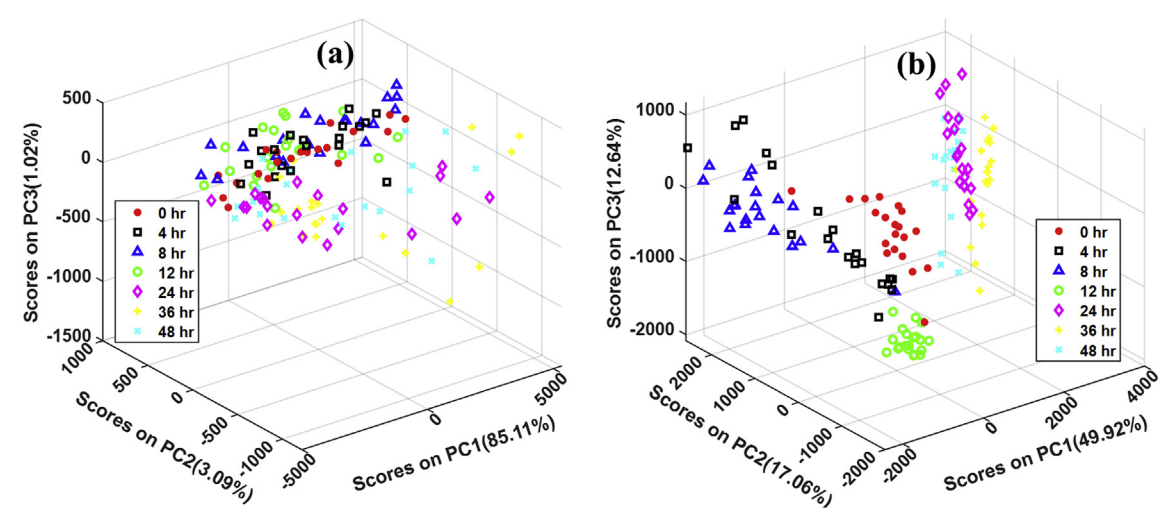


Fig. 5. (a) PCA scatter plot of the SERS spectra of the seven real tuna samples for different spoilage time without TLC and (b) after TLC development.

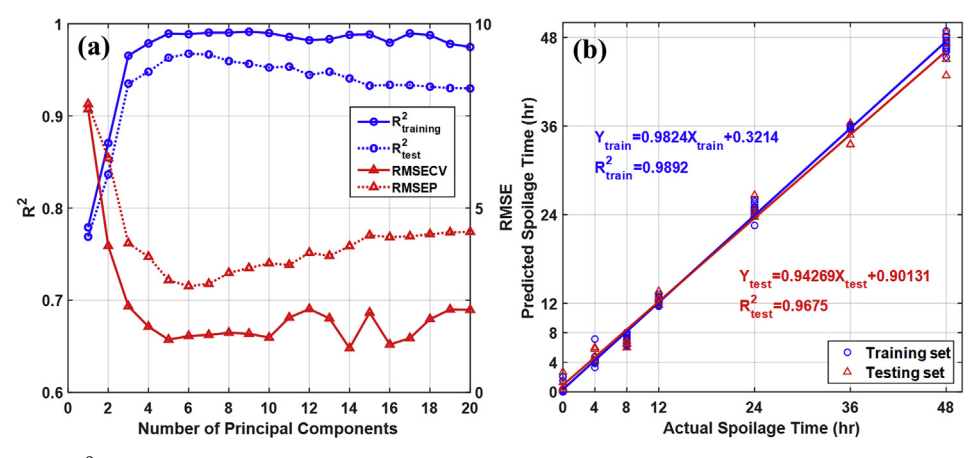


Fig. 6. (a) Relationship between R² and RMSE values with the number of PCs. (b) PCA-SVR calibration curves of the predicted spoilage time and actual spoilage time.

key features and reduce the dimensionality prior to develop a prediction model using SVR algorithm. As shown in the PCA plot in Fig. 5(a), the seven groups of the SERS spectra without TLC development were mixed together and were difficult to distinguish. As a comparison, the principal components (PCs) of the SERS spectra after TLC developing in Fig. 5(b) were clustered with each spoilage time and for each spoilage time dataset, they were well separated from each other. In this analysis, the first three PCs of the SERS spectra account for 89.22% and 79.58% of the variance for the seven groups of spoiled tuna samples without executing TLC and with executing TLC, respectively. The values of 89.22% and 79.58% prove that the first three principal components

account for most of the variance and are sufficient to represent the data by the scattering plots as shown in Fig. 5. The weights of these PCs are PC $_1$ 85.112%, PC $_2$ 3.091%, PC $_3$ 1.02% and PC $_1$ 49.92%, PC $_2$ 17.02%, PC $_3$ 12.64% accordingly.

The basic process of PCA is to project the raw spectra into the principal component coordinates. The values in the scatter plot of Fig. 5, namely the PC scores, are obtained by orthogonal transformation. Clustering of the PCs shown in Fig. 5 (b) indicated that there is some systematic change of the extracted solution from the tuna meat with respect to the spoilage time. For example, the PCs of tuna samples with short spoilage time (0, 4, 8, and 12h) are clearly separated from

Table 1
Comparison of quantitative modeling of real tuna samples with different spoilage time.

Method		PCs Number	Training Set		Testing Set		
			RMSECV	R^2	RMSEP	R^2	RPD
Without TLC	PLSR	n = 5	3.219	0.946	7.379	0.784	1.969
	SVR	n = 8	5.566	0.896	7.600	0.787	1.812
After TLC	PLSR	n = 7	2.142	0.982	4.373	0.933	3.752
	SVR	n = 6	1.531	0.989	2.882	0.968	6.131

the samples with longer spoilage time (24, 36 and 48 h). This indicates the significant difference of the Raman spectra due to the increase of histamine levels. Furthermore, the spoiled samples with different time also form four relatively separated groups: $0\,h$, $4–8\,h$, $12\,h$, and $24–48\,h$, although some dataset may have slight overlap, which is due to the random factors of the TLC-SERS measurement.

After PCA feature extraction, a SVR model was constructed with the training dataset and was further evaluated using a testing dataset. The R² and RMSE values of the training and testing dataset against the number of principal components are presented in Fig. 6 (a). From these plots, it can be found that in the range of five to seven of the number of the principal components, the R² get to the relative maximum values and the RMSE reach the relative minimum values. Therefore, six principal components (capture 86.91% of the variation or information contained in the spectra) were chosen to construct the SVR model. Grid searching method was conducted in the search range $[2^{-10} \ 2^{10}]$ to determine the optimal values for the two key parameters (γ for the RBF kernel and C for the SVR). Various pairs of (C, γ) values were tested and the best parameters pair (64, 4) with the best cross-validation accuracy is picked at last. Based on the optimal model, the calibration curves for the actual spoilage time and predicted spoilage time in both the training and testing sets were shown in Fig. 6(b). It can be seen that the predicted spoilage time was very close to the actual spoilage time for each sample.

We also performed linear PLSR model for comparison and the calibration curves for the actual spoilage time and predicted spoilage time were shown in Fig. S9. Quantitative modeling results obtained by the PLSR and SVR are shown in Table 1. From the comparison of TLC-SERS results, the regression model constructed based on SVR showed much better performance with higher R², RPD and lower RMSECV, RMSEP than those of the PLSR model, which indicates that the SVR model has the better predictive ability. These results were attributed to the fact that the SVR model can grasp more nonlinearities between the SERS spectra and the TLC-SERS procedure. As a comparison, PLSR is inherently a linear modeling method, which makes it difficult to account for the nonlinear relationship. Interestingly, SVR shows comparable or even slightly worse performance than PLSR for the SERS only measurement without performing TLC, which means TLC separation is a necessary technique for machine learning analysis.

4. Conclusions

In this study, we have developed a quantitative TLC-SERS sensing method to detect histamine from artificial and real spoiled tuna samples with SVR analysis. The diatomaceous earth TLC plates used herein not only separate histamine from complex tuna meat matrix, but also serve as ultra-sensitive SERS substrates to enhance the detection limit down to 10 ppm, which is far below the 50 ppm safety level set by US FDA. In addition, we applied the TLC-SERS sensing techniques to detect histamine from real spoiled tuna samples. Using the PCA-SVR algorithm to analyze the SERS spectra, we are able to build an accurate quantitative model to evaluate the histamine level with respect to the spoilage time in real tuna samples. Considering that TLC is one of the low cost analytical chemistry methods and the affordability of portable Raman

spectrometers, the reported SVR-enabled TLC-SERS sensor would enable a rapid, cost-effective, and quantitative on-site detection technique for histamine in seafood. From an even broader sense, the developed method proves that a cost-effective TLC-SERS technique, which are rapid but suffer low sensitivity and can only perform qualitative sensing, can be transformed into a sensitive, accurate, and quantitative sensing technique through machine-learning methods. It may also open the gates for many other chemical and biological sensing applications such as drug detection, water quality measurement, and homeland security.

Acknowledgements

The authors would like to acknowledge the support from the National Institutes of Health under Grant No. 1R21DA0437131, the Unites States Department of Agriculture under Grant No. 2017- 67021-26606 and the National Science Foundation under Grant No. 1701329. A. Tan and Y. Zhao would also like to acknowledge the support from China Scholarship Council.

Appendix A. Supplementary data

Supplementary data to this article can be found online at https://doi.org/10.1016/j.foodcont.2019.03.032.

References

- Brosseau, C. L., Gambardella, A., Casadio, F., Grzywacz, C. M., Wouters, J., & Van Duyne, R. P. (2009). Ad-hoc surface-enhanced Raman spectroscopy methodologies for the detection of artist dyestuffs: Thin layer chromatography-surface enhanced Raman spectroscopy and in situ on the fiber analysis. *Analytical Chemistry*, 81, 3056–3062.
- Bulushi, I. A., Poole, S., Deeth, H. C., & Dykes, G. A. (2009). Biogenic amines in fish: Roles in intoxication, spoilage, and nitrosamine formation-A review. *Critical Reviews in Food Science and Nutrition*, 49, 369–377.
- CDC (2006). Scombroid fish poisoning associated with tuna steaks-Louisiana and Tennessee. Morbidity and Mortality Weekly Report, 56(2007), 817–819.
- Cowcher, D. P., Jarvis, R., & Goodacre, R. (2014). Quantitative online liquid chromatography- surface-enhanced Raman scattering of purine bases. *Analytical Chemistry*, 86, 9977–9984.
- Craig, A. P., Franca, A. S., & Irudayaraj, J. (2013). Surface-enhanced Raman spectroscopy applied to food safety. Annual Review of Food Science and Technology, 4(1), 369–380.
- Davis, K. L., McGlashen, M. L., & Morris, M. D. (1992). Surface-enhanced Raman scattering of histamine at silver electrodes. *Langmuir*, 8, 1654–1658.
- Dong, R. L., Weng, S. Z., Yang, L. B., & Liu, J. H. (2015). Detection and direct readout of drugs in human urine using dynamic surface-enhanced Raman spectroscopy and support vector machines. *Analytical Chemistry*, 87(5), 2937–2944.
- EC (2005). Commission regulation (EC) No. 2073/2005 on microbiological criteria for foodstuffs. L 338/1. Official Journal of the European Union.
- FDA (2011). Scombrotoxin (histamine) formation in fish and fishery products hazards and controls guidance. Department of health and human services, public health service, food and drug administration, center for food safety and applied nutr. (4th ed.). Washington, DC, USA: Office of Food Safety.
- Feng, C., Teuber, S., & Gershwin, M. E. (2016). Histamine (scombroid) fish poisoning: A comprehensive review. Clinical Reviews in Allergy and Immunology, 50, 64–69.
- Freye, C. E., Crane, N. A., Kirchner, T. B., & Sepaniak, M. J. (2013). Surface enhanced Raman scattering imaging of developed thin-layer chromatography plates. *Analytical Chemistry*, 85(8), 3991–3998.
- Gao, F., Grant, E., & Lu, X. (2015). Determination of histamine in canned tuna by molecularly imprinted polymers-surface enhanced Raman spectroscopy. *Analytica Chimica Acta*, 901, 68–75.
- Gao, F., Hu, Y., Chen, D., Li-Chan, E. C. Y., Grant, E., & Lu, X. (2015). Determination of Sudan I in paprika powder by molecularly imprinted polymers-thin layer chromatography-surface enhanced Raman spectroscopic biosensor. *Talanta*, 143, 344–352.
- Grabar, K. C., Freeman, R. G., Hommer, M. B., & Natan, M. J. (1995). Preparation and characterization of Au colloid monolayers. *Analytical Chemistry*, 67, 735–743.
- Gukowsky, J. C., Xie, T., Gao, S. Y., Qu, Y. Q., & He, L. L. (2018). Duyne. Rapid identification of artificial and natural food colorants with surface enhanced Raman spectroscopy. Food Control, 92, 267–275.
- He, L., Rodda, T., Haynes, C. L., Deschaines, T., Strother, T., Diez-Gonzalez, F., et al. (2011). Detection of a foreign protein in milk using surface-enhanced Raman spectroscopy coupled with antibody-modified silver dendrites. *Analytical Chemistry*, 83(5), 1510–1513.
- Huang, R. F., Han, S. Y., & Li, X. (2013). Detection of to bacco-related biomarkers in urine samples by surface-enhanced Raman spectroscopy coupled with thin-layer chromatography. *Analytical and Bioanalytical Chemistry*, 405, 6815–6822.
- Hu, X. P., Fang, G. Z., Han, A. L., Liu, J. M., & Wang, S. (2017). Rapid detection of Pericarpium papaveris in hot pot condiments using thin-layer chromatography and

- surface enhanced Raman spectroscopy combined with a support vector machine. *Analytical Methods, 9,* 2177–2182.
- Janči, T., Valinger, D., Kljusurić, J. G., Mikac, L., Vidaček, S., & Ivanda, M. (2017). Determination of histamine in fish by Surface Enhanced Raman Spectroscopy using silver colloid SERS substrates. Food Chemistry, 1(224), 48–54.
- Jarvis, R. M., Brooker, A., & Goodacre, R. (2004). Surface-enhanced Raman spectroscopy for bacterial discrimination utilizing a scanning electron microscope with a Raman spectroscopy interface. *Analytical Chemistry*, 76(17), 5198–5202.
- Karaballi, R. A., Nel, A., Krishnan, S., Blackburn, J., & Brosseau, C. L. (2015). Development of an electrochemical surface-enhanced Raman spectroscopy (EC-SERS) aptasensor for direct detection of DNA hybridization. *Physical Chemistry Chemical Physics*, 17, 21356–21363.
- Kong, X., Chong, X., Squire, K., & Wang, A. X. (2018). Microfluidic diatomite analytical devices for illicit drug sensing with ppb-Level sensitivity. Sensors and Actuators B: Chemical. 259, 587–595.
- Kong, X., Li, E., Squire, K., Liu, Y., Wu, B., Cheng, L. J., et al. (2017a). Plasmonic nanoparticles-decorated diatomite biosilica: Extending the horizon of on-chip chromatography and label-free biosensing. *Journal of Biophotonics*, 10, 1473–1484.
- Kong, X., Squire, K., Chong, X., & Wang, A. X. (2017b). Ultra-sensitive lab-on-a-chip detection of Sudan I in food using plasmonics-enhanced diatomaceous thin film. Food Control, 79, 258–265.
- Kong, X., Squire, K., Li, E., LeDuff, P., Rorrer, G. L., & Tang, S. (2016). Chemical and biological sensing using diatom photonic crystal biosilica with in-situ growth plasmonic nanoparticles. *IEEE Transactions on NanoBioscience*, 15, 828–834.
- Kong, X., Xi, Y., LeDuff, P., Chong, X., Li, E., Ren, F., et al. (2017c). Detecting explosive molecules from nanoliter solution: A new paradigm of SERS sensing on hydrophilic photonic crystal biosilica. *Biosensors and Bioelectronics*, 88, 63–70.
- Krooshof, P. W. T., Üstün, B., Postma, G. J., & Buydens, L. M. C. (2010). Visualization and recovery of the (Bio)chemical interesting variables in data analysis with support vector machine classification. *Analytical Chemistry*, 82(16), 7000–7007.
- Li, D., Li, D. W., Fossey, J. S., & Long, Y. T. (2010). Portable surfaceenhanced Raman scattering sensor for rapid detection of aniline and phenol derivatives by on-site electrostatic preconcentration. *Analytical Chemistry*, 82, 9299–9305.
- Li, D. W., Qu, L. L., Zhai, W. L., Xue, J. Q., Fossey, J. S., & Long, Y. T. (2011). Facileon-sitedetection of substitute daromatic pollutants in water using thin layer chromatography combined withsurface-enhanced Raman spectroscopy. *Environmental Science & Technology*, 45, 4046–4052.
- Liu, Y., & Lu, F. (2017). Adulterated pharmaceutical chemicals in botanical dietary supplements: Novel screening approaches. *Reviews in Analytical Chemistry*, 36(3), 1–14.
- Losic, D., Mitchell, J. G., & Voelcker, N. H. (2009). Diatomaceous lessons in nanotechnology and advanced materials. Advanced Materials Interfaces, 21, 2947–2958.
- Losic, D., Rosengarten, G., Mitchell, J., & Voelcker, N. (2006). Pore architecture of diatom frustules: Potential nanostructured membranes for molecular and particle separations. *Journal of Nanoscience and Nanotechnology*, 6, 982–989.
- Lucotti, A., Tommasini, M., Casella, M., Morganti, A., Gramatica, F., & Zerbi, G. (2012). TLC-surface enhanced Raman scattering of apomorphine in human plasma. Vibrational Spectroscopy, 62, 286–291.
- Lupo, A., & Mozola, M. (2011). Validation study of a rapid ELISA for detection of

- histamine in tuna. Journal of AOAC International, 94, 886-899.
- Lv, D. Y., Cao, Y., Lou, Z., Li, S., Chen, X., Chai, Y., et al. (2015). Rapid on-site detection of ephedrine and its analogues used as adulterants in slimming dietary supplements by TLC–SERS. Analytical and Bioanalytical Chemistry, 407, 1313–1325.
- Muscarella, M., Lo Magro, S., Campaniello, M., Armentano, A., & Stacchini, P. (2013).
 Survey of histamine levels in fresh fish and fish products collected in Puglia (Italy) by
 ELISA and HPLC with fluorimetric detection. Food Control, 31(1), 211–217.
- Ohtsubo, Y., Kurooka, H., Tada, H., & Manabe, N. (2014). Method for determination of histamine in food by LC-MS/MS. Food Hygiene and Safety Science, 55, 103–109.
- Önal, A., Tekkeli, S. E. K., & Önal, C. (2013). A review of the liquid chromatographic methods for the determination of biogenic amines in foods. *Food Chemistry*, 138, 509-515
- Qi, J., Motwani, P., Gheewala, M., Brennan, C., Wolfe, J. C., & Shih, W. C. (2013). Surface-enhanced Raman spectroscopy with monolithic nanoporous gold disk substrates. *Nanoscale*. 5, 4105–4109.
- Radu, A. I., Kuellmer, M., Giese, B., Huebner, U., Weber, K., Cialla-May, D., et al. (2016). Surface-enhanced Raman spectroscopy (SERS) in food analytics: Detection of vitamins B2 and B12 in cereals. *Talanta*, 160, 289–297.
- Ramírez, F. J. I., Collado, T. J. A., & Silla, E. (2003). Structural and vibrational study of the tautomerism of histamine free-base in solution. *Journal of the American Chemical* Society, 125, 2328–2340.
- Tao, Z., Sato, M., Han, Y., Tan, Z., Yamaguchi, T., & Nakano, T. A. (2011). Simple and rapid method for histamine analysis in fish and fishery products by TLC determination. Food Control, 22, 1154–1157.
- Tarliane, M. S., Priscila, S. S., Warlley, P. E., & Maria Beatriz, A. G. (2011). Occurrence of histamine in Brazilian fresh and canned tuna. Food Control, 22(2), 323–327.
- Wu, Z. Z., Xu, E. B., Long, J., Wang, F., Xu, X. M., et al. (2015). Measurement of fermentation parameters of Chinese rice wine using Raman spectroscopy combined with linear and non-linear regression methods. *Food Control*, 56, 95–102.
- Xie, Z., Wang, Y., Chen, Y., Xu, X., Jin, Z., Ding, Y., et al. (2017). Tuneable surface enhanced Raman spectroscopy hyphenated to chemically derivatized thin-layer chromatography plates for screening histamine in fish. Food Chemistry, 230, 547–552.
- Xu, X., Li, H., Hasan, D., Ruoff, R. S., Wang, A. X., & Fan, D. L. (2013). Near-field enhanced plasmonic-magnetic bifunctional nanotubes for single cell bioanalysis. Advanced Functional Materials, 23, 4332–4338.
- Yu, W., & White, I. M. (2013). Chromatographic separation and detection of target analytes from complex samples using inkjet printed SERS substrates. *Analyst*, 138, 3679–3686.
- Zhang, N., Liu, K., Liu, Z. J., Song, H. M., Zeng, X., Ji, D. X., et al. (2015). Ultrabroadband metasurface for efficient light trapping and localization: A universal surface-enhanced Raman spectroscopy substrate for "all" excitation wavelengths. Advanced Materials Interfaces. 2(10). 1500142.
- Zhang, Z. M., Liu, J. F., Liu, R., Sun, J. F., & Wei, G. H. (2014). Thin layer chromatography coupled with surface-enhanced Raman scattering as a facile method for on-site quantitative monitoring of chemical reactions. *Analytical Chemistry*, 86(15), 7286–7292.
- Zhu, Q., Cao, Y., Cao, Y., Chai, Y., & Lu, F. (2014). Rapid on-site TLC-SERS detection of four antidiabetes drugs used as adulterants in botanical dietary supplements. *Analytical and Bioanalytical Chemistry*, 406, 1877–1884.